metals

MDPI

Article

Mechanical Strengthening in S235JR Steel Sheets through Vibration-Assisted Ball Burnishing

Jordi Llumà [1], Giovanni Gómez-Gras [2], Ramón Jerez-Mesa [3,*], Jaume Rue-Mascarell [4] and J. Antonio Travieso-Rodriguez [4]

1 Materials Science and Metallurgical Engineering Department, Escola d'Enginyeria de Barcelona Est, Universitat Politècnica de Catalunya, Avinguda d'Eduard Maristany, 10-14, 08019 Barcelona, Spain; jordi.lluma@upc.edu
2 Institut Químic de Sarrià School of Engineering, Via Augusta, 390, 08017 Barcelona, Spain; giovanni.gomez@iqs.edu
3 Engineering Department, Faculty of Sciences and Technology, Universitat de Vic—Universitat Central de Catalunya, C. Laura, 13, 08500 Vic, Spain
4 Mechanical Engineering Department, Escola d'Enginyeria de Barcelona Est, Universitat Politècnica de Catalunya, Avinguda d'Eduard Maristany, 10-14, 08019 Barcelona, Spain; jaume.rue@estudiant.upc.edu (J.R.-M.); antonio.travieso@upc.edu (J.A.T.-R.)
* Correspondence: ramon.jerez@uvic.cat; Tel.: +34-938-815-519

Received: 6 July 2020; Accepted: 24 July 2020 ; Published: 28 July 2020

Abstract: The superficial effect of hardening caused after vibration-assisted ball burnishing and its consequences in the tensile behavior of a carbon steel material are studied in this paper. As ball burnishing affects the material to hundredths of micrometers in depth through plastic deformation, the overall macro effect of this modification was studied. Different levels of preload and vibration amplitude were studied to address the described issue. The study was done in two phases. First of all, the depth to which ball burnishing affects the material was studied by performing Vickers indentation tests with different loads. It was proven that the effects of ball burnishing are best represented when a 0.05 kg load is used, as higher loads include more volume of core material in the measurement, hence hiding the effect of ball burnishing. In a second phase, the ball burnished specimens were subjected to tensile tests. It was proven that an increase of burnishing preload diminishes the ductile behavior of the material and increases its strength representative values, although the proportion of affected material in the cross-section of the specimen is reduced with regard to the whole surface. Additionally, as the preload increases, the effects of assistance through vibrations is reduced, and the effect of the static preload acquires more relevance in modifying the macroscopic mechanical properties of the steel alloy. Experiments using different amplitudes and new forces are encouraged to obtain more information about how the material can be modified optimally through vibration-assisted ball burnishing.

Keywords: tensile strength; ball burnishing; vibration-assistance; mechanical properties; hardness

1. Introduction

The enhancement of the properties of materials is a field of scientific interest in continuous evolution. Engineering applications require materials with stable properties, configured in shapes and as workpieces with enhanced surface integrity and good states for the alloys that confirm them. An increased bearing capacity or strength-to-weight ratio, along with lengthened fatigue lifespans and weight lightening without rigidity loss, are just some of the characteristics that are expected from new generation materials. Excellent mechanical properties of workpieces must be guaranteed by means of mastering the processes by which surface characteristics are modified [1]. For these reasons,

the study of the effects of finishing processes to guarantee stability of their effects, and to achieve a good traceability to succeed in implementing them in production lines is basic in this sense [2]. In this framework, ball burnishing has been positioned by many authors, and also in actual industrial applications, as a very good candidate to achieve this material enhancement [3]. Ball burnishing (BB) is a cold deformation process that consists of plastic deformation of the peaks of a surface texture because of the pressure exerted by a ball or a roller [4]. As a direct consequence of the process characteristics, compressive residual stresses are induced on the surfaces, which guarantees the improvement of many of the features that have been explained above, and that are demanded from materials [5]. Furthermore, it also provides clear advantages in terms of productivity because burnishing tools can be perfectly integrated in the manufacturing process due to the fact that the process does not need a special machine to be executed. It can be done in the same milling or turning machine where the machining routine to generate the workpiece geometry has been performed. This is a clear advantage of the process compared to other traditional finishing processes, such as shot peening or polishing [6].

Current research lines focus on studying the effects of ball burnishing in diverse industrial sectors, such as transportation engineering, machine components and mold manufacturing. This increasing interest has also boosted the introduction of elements that improve the results obtained by means of the conventional process. For instance, vibration assistance is one of the ways with which to improve a process with robust and stables systems [7]. Its beneficial effects have been reported in several previous experimental applications, both in realizations wherein assistance is ultrasonic [8] and wherein it takes the form of sonic frequencies [9]. The physical effect of vibration assistance on ball burnishing can be explained by the fact that it provokes an acoustoplastic effect on the material lattice; that is, it facilitates dislocation traveling all over the atomic lattice, facilitating plastic deformation on a macroscopic scale [10].

A variable residual effect on hardness can also be expected after the application of the process, depending on various factors, such as the vibration amplitude or frequency, or the material on which it is applied [11]. For that reason, the effects of vibration-assisted ball burnishing (VABB) must be assessed on different materials and under different circumstances to understand what the actual implications of the process itself are. However, today we know that VABB on carbon steel alloys delivers more positive results than its non-assisted counterpart, increasing the depth of affectation of the treated surface [12] and improving the rolling movement of the burnishing ball, which prevent damage of the objective surface [13]. Results are also positive on other alloys, such as A92017-T4 [14].

Of all descriptors that can describe the state of an engineering surface, some of them evidence more affectation through VABB. Surface hardness is one of them. According to Saldaña-Robles et al. (2018), residual hardness after VABB on AISI 1045 surfaces is increased up to 60% [15]. Similar results were obtained on G10380 steel surfaces by Travieso-Rodríguez (2015) [16]. Specifically, in VABB, a higher frequency should be recommended to obtain the highest residual hardening effect. Pande et al. (1984) confirmed this observation on C20 steel, determining that 40 kHz was the best frequency to assist the process [17]. Surface roughness is also usually focused on to evaluate the effects of ultrasonic vibration-assisted ball burnishing (UVABB). Pak et al. (2020) tested a 20-kHz VABB process on A6061-T6 aluminum specimens and proved that roughness is affected by the vibration amplitude [18]. Specifically, it should be as low as possible to obtain lower *Ra* values. Teimouri et al. (2018) fixed a maximum value of amplitude at 5 μm to guarantee that the process was not detrimental in terms of roughness, at the sight of results obtained on the same aluminum alloy [19]. This is also true in steel alloys, according to other authors [17].

The effects of VABB have been studied on both flat and cylindrical surfaces. Rodríguez et al. (2012) stated that, on revolution workpieces, VABB can reduce the *Ra* to 0.3 μm and increase residual hardness in 60% [20]. The effects of ultrasonic VABB were also studied by Huuki et al. (2014) on different cylindrical specimens made of aluminum, tempered steel and structural steel alloys [21]. The authors also reported that both hardness and roughness are visibly enhanced through VABB, and that the degree of improvement is independent of the material of the specimen.

It is also worth mentioning that similar improvements are obtained regardless of the burnishing element geometry. In the studies presented by Lu et al. (2016), low-hardness A7050-T7451 aluminum steel was burnished with a roller. X-ray diffraction and spectrometry techniques evidenced that the process successfully enhanced surface integrity, as microhardness was increased and roughness was reduced [22].

This work aims to present the results of VABB on S235JR alloy via analyzing its effects on flat surfaces subjected to tensile tests. As a comparison, specimens burnished with the non-assisted process were manufactured and tested. The stress–strain curves of all of them are represented and were processed to obtain the mechanical descriptors of all ball burnishing conditions. The relevance of this study is the lack of similar studies about S235JR steel. This alloy is especially used as a constructive and structural material in industry, hence the interest of knowing the effects of the process on its mechanical properties for future eventual implementations.

2. Experimental Approach

2.1. Methodology

To validate the effects of ball burnishing on the tensile behavior and surface hardening of S235JR steel (UNE EN 10027-1), tensile specimens according to the UNE-EN ISO 6892-1 standard were manufactured and ball-burnished during this experimental campaign. These parts were then subjected to different tests with the aim of determining various mechanical properties of the material after surface modification through VABB. Specifically, surface hardness, yield strength, maximum strength, maximum elongation, resilience module and the different coefficients that characterize the material hardening were computed by extracting them from different stress–strain curves.

During the first stage of the experimental procedure, specimens were burnished applying different conditions. For each combination of burnishing parameters, three specimens were tested to corroborate the repeatability of the results. In a second stage, indentation tests were performed on the flat surfaces of the parts in order to determine how the Vickers microhardness of the material varied according to the indentation load. That way, a hardness profile depending on the depth of penetration of the indenter was constructed. In a third phase, the same specimens were the objects of standard tensile tests to determine the mechanical properties described above. All tests were recorded with a full HD camera, after we had painted all specimens to generate a random pixel-like pattern on their surfaces. This allowed the application of image processing to compute through correlation routines the displacement of all points of the specimen, and from that, the deformation experienced by the material. Last of all, the derived stress–strain curves were processed to compute the main mechanical properties that evidence how the material's behavior changed after being subjected to ball burnishing. The experimental design followed to obtain the different burnishing conditions is explained in subsequent subsections.

2.2. Specimen Preparation

The dogbone specimens used in this study were manufactured by laser machining the desired profile on a S235JR hot rolled plate with a thickness of 2 mm. The chemical composition is indicated in Table 1. Their shape and dimensions are 105 mm length and 10 mm width, according to the UNE-EN ISO 6892-1:2017 standard. This material was chosen because of its use as structural steel and its high abundance in the industry for various applications in different fields.

Table 1. Chemical composition of S235JR steel.

Element	C	Si	Mn	P	S	Cr	Ni
% weight	0.11	0.03	0.056	0.007	0.005	0.07	0.03

Due to the characteristics of the cutting process used to shape the specimens, a certain dimensional variability can be expected. This fact could introduce a source of variability that could significantly affect the bearing sections of all of them. For this reason, a previous metrology phase was introduced into the process, consisting of three measurements of the thicknesses and widths of the specimens, thereby obtaining average cross-sections and standard deviations, confirming that all of the latter were contained inside the measurement error, and were, therefore, acceptable.

The described specimens were attached to the milling machine by means of an epoxy equipment machined *ad hoc* to fit three specimens per fixation (Figure 1). By doing this, it was guaranteed that all specimens are modified equally during the process, and that all of them were oriented regularly with regard to the standard burnishing direction. All three specimens installed at a single time were treated by applying the same conditions.

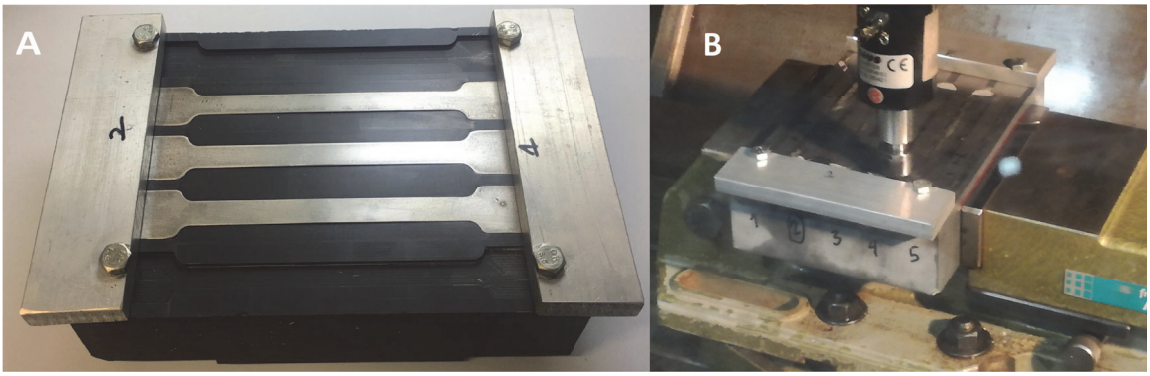

Figure 1. (**A**) Three tensile specimens fitted in the epoxy equipment. (**B**) Burnishing tool while treating the specimens.

2.3. Ball Burnishing Setup

2.3.1. Ball Burnishing Tool

The tool used for this was designed and characterized by Jerez-Mesa et al. (2018) [23]. The tool is equipped with a piezoelectric transducer that resonates mechanically to a 40-kHz alternate voltage by means of an external power circuit. The tool can execute the assisted process when that circuit is turned on, whereas the conventional non-assisted process is performed when it is off. The vibratory movement is amplified by a sonotrode, so that the ball supported on its end vibrates with a 10 µm amplitude when it is unloaded on a target surface. The 10 mm diameter burnishing ball is able to roll freely during the process and is made of 100Cr6 chrome steel (according to UNE EN 10027-1 standard).

2.3.2. Burnishing Preload

Previous studies have evidenced that the burnishing preload is the most influential factor on the degree of plastic deformation achieved after a BB process, regardless of the material being treated [24,25]. For this reason, it was chosen as a factor to be included in this study. It can be expected that for a low carbon steel like the one that was tested, 90, 150 and 260 N can provide sufficient variation to study the influence in the response.

2.3.3. Vibration Amplitude

Previous studies have also shown that vibration-assistance reduces shear forces during the application of ball burnishing, and also contributes positively by increasing the extent to which plastic deformation is applied on the surface irregularities, due to the acoustoplastic effect that vibrations cause. As the power circuit that excites the piezoelectric stack allows the adjustment of the amplitude of the vibration, it was decided to work with three different amplitudes in this experimental campaign:

100% (or ±10 µm free amplitude), 50% (±5 µm free amplitude), and 0%, meaning that no vibration assistance was put in place.

2.3.4. Experimental Design

To analyze first and second-order influences of the factors on the tensile responses of the specimens, a full factorial design was selected to combine all parameters and levels. Table 2 shows the two parameters chosen to be varied and their three different levels. Consequently, 9 different experimental conditions were derived from this experimental design, and provided that 3 repetitions were tested for each of them, a total of 27 specimens were burnished and later on subjected to tensile tests. For the obtained results, three more untreated specimens were also subjected to tensile tests to establish a comparison point and evaluate the effect of ball burnishing on the raw material.

Table 2. Parameters considered in the experimental design and their values.

Parameter	Levels		
	I	**II**	**III**
Burnishing force, F (N)	90	150	260
Vibration amplitude, A (%)	0	50	100

2.3.5. Other Parameters

Further parameters that affect the application of ball burnishing have been kept constant, considering results obtained after previous works [25]. Table 3 shows these values. Only one pass was performed on the material because the effect of more passes is similar to increasing the burnishing force, so that the eventual change in the response can be fully accounted for by the force variation.

Table 3. Parameters kept constant during the experimental execution.

Feed Velocity v_a (mm/min)	**Lateral Offset between Passes b (mm)**	**Number of Passes N**
900	0.25	1

2.4. Response Indicators

2.4.1. Microhardness Measurement

The hardening effect induced on the material's surface was studied in this work by performing different Vickers tests (according to UNE EN ISO 6507-1) while varying the indentation load for each burnishing condition. A microhardness indenter machine Micromet 5114 (Buehler, Chicago, IL, USA) has been used. Five different loads, namely, 0.025 kg, 0.05 kg, 0.2 kg, 1.0 kg and 2.0 kg were applied, so that with each one, an increasingly higher depth was achieved during the test, and a higher proportion of the core material was taken into consideration for the hardness measurement (Figure 2). The generated profiles allow the observation and comparison of how the hardening effect is actually performed on the surface. Three repetitions for each specimen and burnishing condition were carried out and averaged.

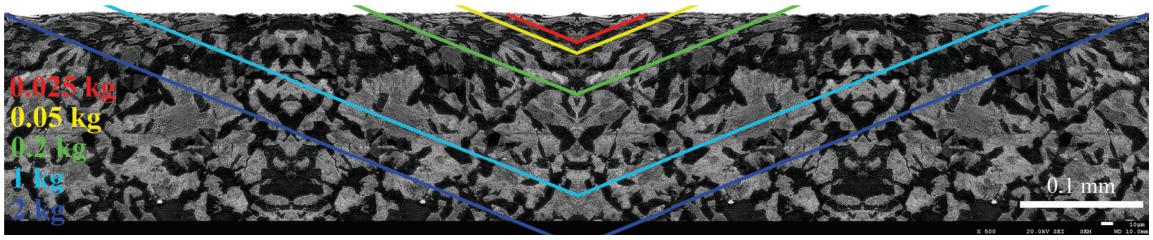

Figure 2. Schematic representation of the penetration achieved with the indentations with different loads on the tested steel, based on real experimental values.

2.4.2. Tensile Testing

Tensile tests were undertaken with a universal electromechanical testing machine EM2/20 (Microtest, Madrid, Spain) at room temperature. The force acquisition was performed through a 25-kN load cell HBM U10M of class 0.03. As the S235JR steel is very ductile, nominally able to reach deformations of up to 25% before break, the testing speed was set up at 5 mm/min for all specimens. The tests were also recorded with a full high definition (FHD) camera with 59.94006 fps, so that deformations could be later on computed by digital image correlation (DIC). Specifically, that was performed by detecting the displacement of all dots that compose a random pattern painted on the surface of the specimen by a Matlab routine (Figure 3).

Figure 3. Painted specimen with random pattern for the calculation of deformations.

3. Results and Discussion

3.1. Microhardness Measurement

Considering the average values of the three specimens measured for each burnishing condition, the evolution of hardness with regard to the indentation load is represented in Figure 4. It can be observed that the vibration assistance of the process causes in general a lower residual hardening effect. Specifically, by assisting with a 50% amplitude, the effect is more conspicuous compared to 100%. As the indentation load increases, the effect is less evident, as could be expected, due to the fact that more base material is considered in the indentation measurement. Ideally, all measurements should converge at the same hardness level, as the load increases, because a considerable amount of core material included in the indentation should conceal the effect of a comparatively thin layer affected by ball burnishing. In any case, all burnishing conditions resulted in a positive effect when compared to the untreated material, except with a 90 N and 50% combination, which was clearly unable to modify the original surface.

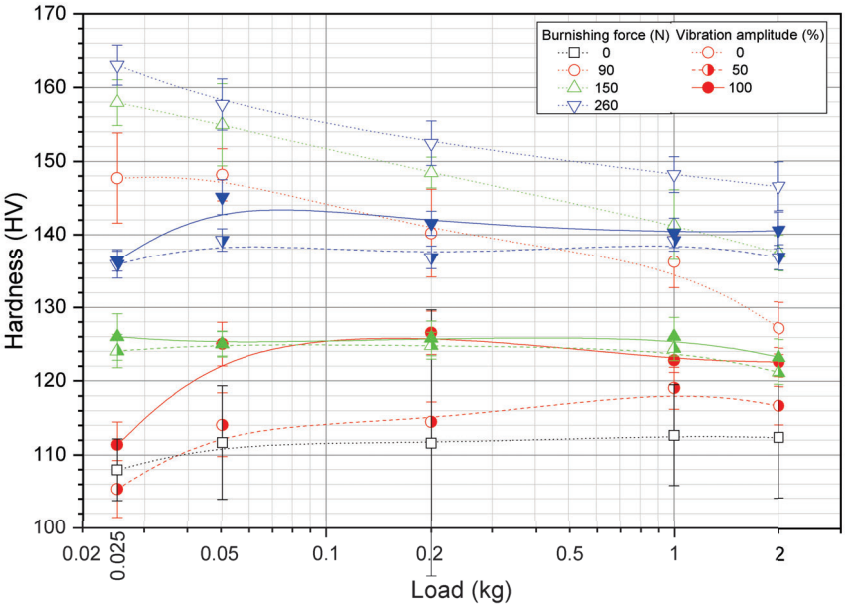

Figure 4. Vickers hardness vs. indentation load for each burnishing condition.

In order to define whether the two factors varied in the experimental application are statistically influential in the evolution of hardness, Figure 5 shows how the standardized effect of each response is affected as a function of the indentation load, with a 95% level of confidence. It can be observed that the significance level of all parameters increases as the indentation load decreases in general, which could be expected because ball burnishing affects only the most superficial grains of the material, and therefore, its effect is more conspicuous in those tests wherein the indenter penetrates less into the material. As the indentation load increases, more unaffected material is involved in the measurement, thereby reducing the significance of all parameters. The only exception is the 25 g load results, in which the indentation imprint is smaller, which therefore implies a higher experimental error implicated in the measurements, and hence the reduction of significance.

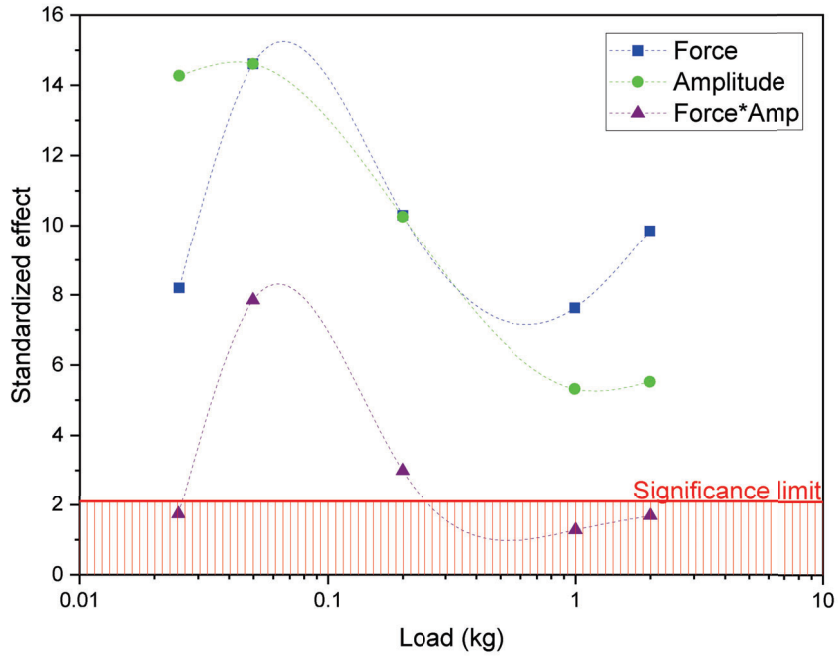

Figure 5. Standardized effect of all parameters vs. Vickers indentation load.

At the sight of the results, one can see that both the force and the amplitude are statistically influential. Additionally, an indentation load of 0.05 kg seems to deliver the most representative results to quantify the effect of ball burnishing, while delivering a low experimental error in the indentation measurement phase. On the other hand, the second-order interaction between the parameters seems to be only significant with that load or 0.2 kg, as is discussed in the next paragraph.

An analysis of variance of all results allows the representation of the mean effect graphs for the hardness measurements for all indentation loads (Figure 6A,B). The burnishing preload positively influences the level of hardening after the application of ball burnishing. This observation agrees with previous conclusions arising from works such as the one developed by Pande and Patel (1984) [17]. Additionally, as it increases, the depth to which the effects are observed also increases, and the effect of ball burnishing is able to penetrate to a higher extent. On the other hand, it is worth mentioning that this hardening effect has a limit, and therefore the effect tends to stabilize at that value asymptotically. Figure 6C shows the direction in which the interaction is oriented. As the preload increases, the effect of the vibration-assistance on the resulting hardness is softened. That is, the increase of the preload gains relevance and is more responsible for the metallurgical change of the material on the subsurface layers, and vibration assistance (at the levels of amplitude tested) loses relevance.

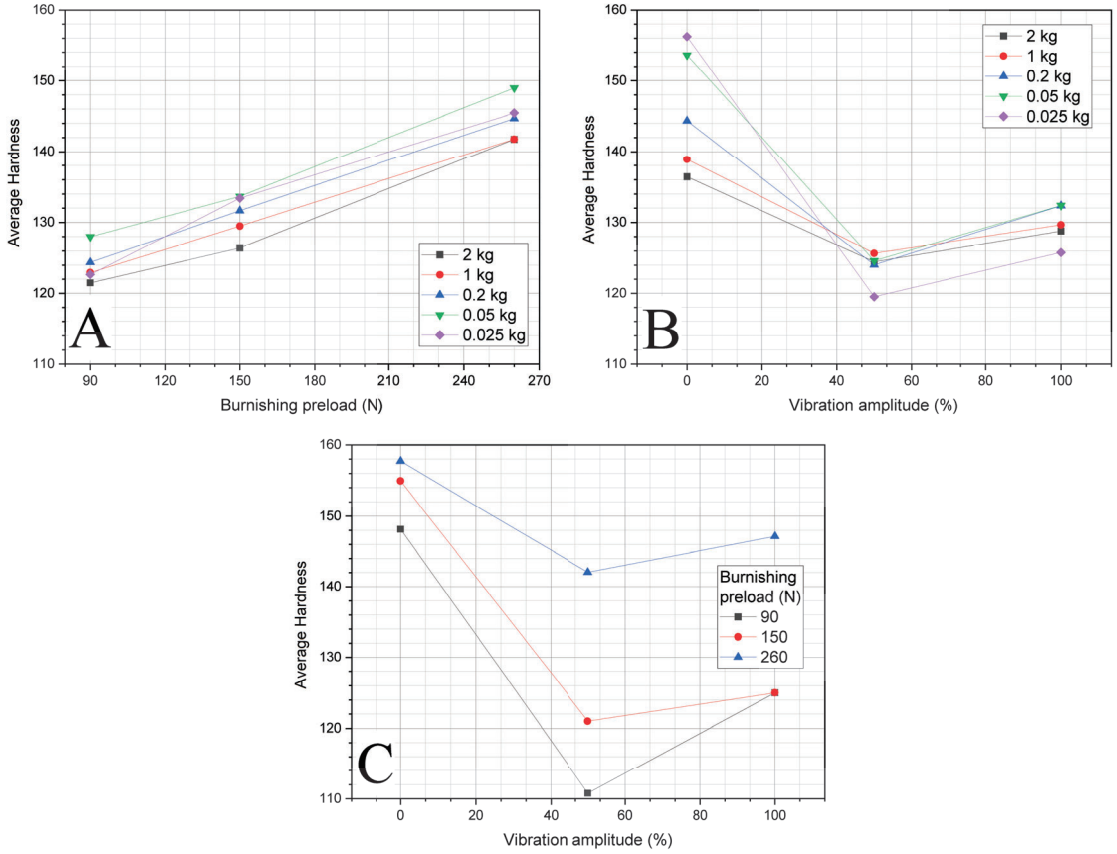

Figure 6. Main effects graphs. Response variable: Vickers hardness. (**A**) Effect of burnishing preload. (**B**) Effect of vibration amplitude. (**C**) Effect of the interaction between the preload and amplitude.

The evolution of hardening as the factors of study evolve can be adjusted to an empirical exponential equation (Equation (1)), regardless of the load used to perform the indentation tests. In all cases, the correlation factor is $R^2 \geq 0.91$.

$$H = H_0 - \Delta H^{\frac{-F}{e^{a+bA+cA^2}}} \quad (1)$$

where H is the Vickers hardness; F is the burnishing preload; A is the percentual amplitude; and H_0, ΔH, a, b and c are coefficients that depend on the load applied in the indentation tests (Table 4).

Table 4. Experimental coefficients of the model representing hardness.

Load (kg)	H_0	ΔH	a	b	c	R^2
2	189 ± 167	-82 ± 159	350 ± 1028	10 ± 26	-0.08 ± 0.22	0.913
1	156 ± 21	-48 ± 18	121 ± 143	5 ± 4	-0.04 ± 0.04	0.936
0.2	155 ± 12	-54 ± 13	71 ± 64	6 ± 4	-0.05 ± 0.03	0.954
0.05	161 ± 16	-57 ± 18	63 ± 67	7 ± 5	-0.05 ± 0.04	0.913
0.025	166 ± 15	-62 ± 16	74 ± 77	9 ± 5	-0.07 ± 0.05	0.961

3.2. Tensile Testing

The stress–strain curves depicted in Figure 7 show that the influence of the burnishing preload is much greater than that of the vibration amplitude. More specifically, as the preload increases, the behavior of the material is more resistant and less ductile. This result is very relevant, if it is considered that this change in the behavior has only been attained by deforming a few micrometres of the surface of the specimen.

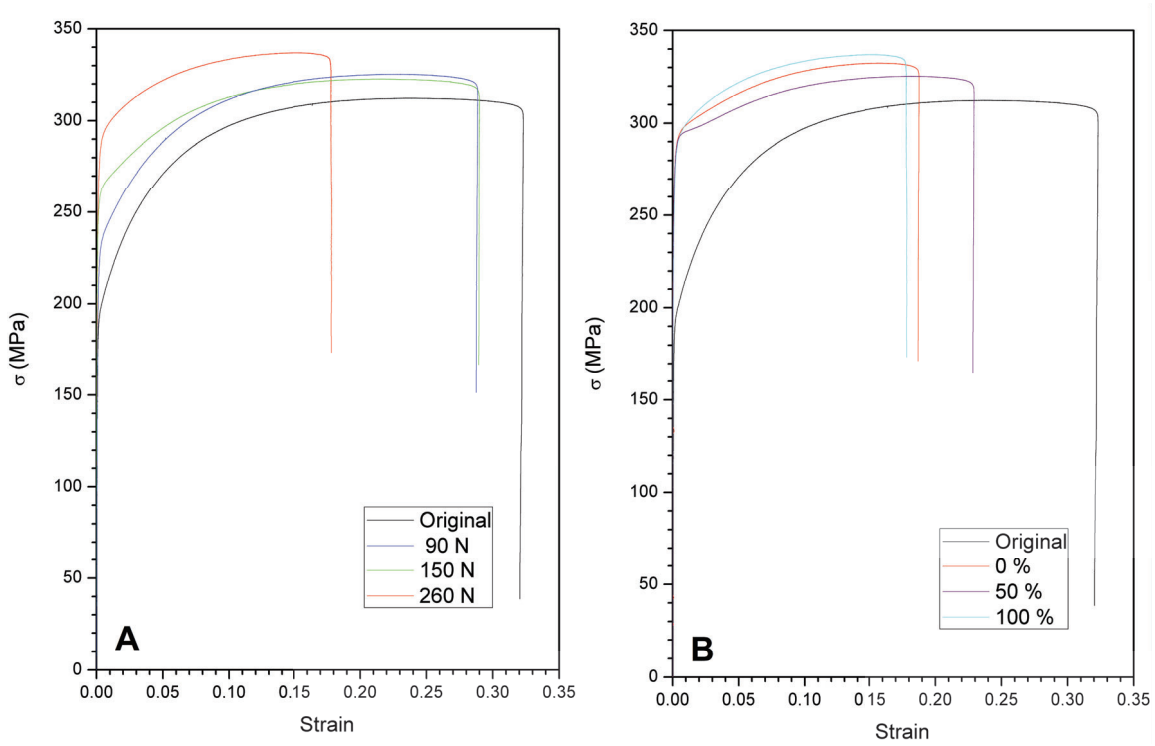

Figure 7. Stress–strain curves of the material showing the effects of both parameters. (**A**) Effect of preload with a 100% amplitude. (**B**) Effect of amplitude with a 260 N preload.

The plastic zones of all curves before the necking of the specimens can be adjusted with a Ludwik hardening model (Equation (2)).

$$\sigma = \sigma_0 + k\epsilon_p \tag{2}$$

where σ is the stress, σ_0 is the yield stress, k is the strength index, ϵ_p is the plastic strain and n is the strain hardening exponent (Table 5).

Table 5. Mechanical properties and their standard deviations calculated from the stress–strain curves.

F (N)	A (%)	$Rp_{0.2}$ (MPa)	UTS (MPa)	e_{UTS} (%)	RM (MPa)	σ_0 (MPa)	k (MPa)	n
0	0	203 ± 6	320 ± 8	0.23 ± 0.02	0.50 ± 0.02	17 ± 15	527 ± 14	0.21 ± 0.01
90	0	225 ± 8	318 ± 6	0.24 ± 0.01	0.56 ± 0.05	158 ± 20	402 ± 21	0.35 ± 0.04
90	50	233 ± 4	322 ± 2	0.21 ± 0.01	0.58 ± 0.05	144 ± 8	410 ± 5	0.31 ± 0.01
90	100	228 ± 6	318 ± 7	0.22 ± 0.02	0.59 ± 0.02	116 ± 63	430 ± 55	0.29 ± 0.09
150	0	232 ± 7	318 ± 6	0.19 ± 0.03	0.63 ± 0.26	176 ± 17	376 ± 15	0.35 ± 0.01
150	50	245 ± 1	328 ± 3	0.20 ± 0.01	0.67 ± 0.01	182 ± 19	382 ± 16	0.35 ± 0.02
150	100	251 ± 8	321 ± 3	0.21 ± 0.01	0.68 ± 0.08	211 ± 11	356 ± 7	0.42 ± 0.03
260	0	278 ± 6	330 ± 3	0.19 ± 0.04	0.72 ± 0.29	249 ± 17	343 ± 15	0.49 ± 0.03
260	50	285 ± 7	328 ± 3	0.17 ± 0.01	0.84 ± 0.11	260 ± 25	326 ± 5	0.52 ± 0.10
260	100	285 ± 9	330 ± 8	0.16 ± 0.02	0.83 ± 0.04	255 ± 9	317 ± 14	0.48 ± 0.02

The effects of the amplitude are not especially conspicuous, and agreeing with the hardness results, the effect with a 50% amplitude can be higher than with a 100% one, specifically when the lowest forces are applied. This is the case for the UTS, for which the maximum resistance is attained by executing the process with a 50% amplitude. Nevertheless, a Pareto statistical analysis shows that the effect of vibrations is not statistically significant for any factor, whereas the preload is indeed. The lack of significance of the amplitude was easy to predict, provided that the hardness results already showed that as the preload increased, a higher volume of raw material was included in the indentation measurement, and the variables lost significance. In the case of the tensile testing, all the sections of the specimen worked, and therefore the amplitude lost complete significance. The core material eclipsed the effect of the superficial hardening. Therefore, given previous works, it can be stated that the differential effects delivered by vibration-assistance are only relevant if local effects such as residual stress are considered to report the effects of processing.

Results show that increasing the preload can lead to an improvement of the effects of ball burnishing. A way to confirm this hypothesis is by calculating a quadratic response surface based on the data obtained from the previous analysis. Table 6 shows the maximum values obtained after an optimization procedure. The only property that increases as the vibration amplitude is reduced is the elongation at UTS, whereas the rest of them are enhanced by means of the vibration-assisted process. Only the properties describing the mechanical resistance of the material seem to require vibration amplitude lower than 100%.

Table 6. Estimated maximum obtained from a quadratic response surface.

Property	F (N)	A (%)	Estimated Maximum	Compound Desirability
e_{UTS}	90	0	0.22	0.778
k (MPa)	90	100	420	0.662
UTS (MPa)	260	53	332	0.841
$Rp_{0.2}$ (MPa)	260	79	287	0.870
RM (MPa)	260	100	0.84	0.798
n	260	100	0.50	0.734
σ_0 (MPa)	260	100	264	0.917

At sight of these results, ball burnishing could be considered to be performed locally on low thickness plates to modify the properties of the material in specific areas of the workpiece. This could enhance the resistance of parts manufactured through processes that use plates as raw material and that require severe plastic deformation, such as deep drawing, to reduce the critical areas where the material could be broken during processing.

As the maximum amplitude tested in this work was 10 µm, it is encouraged to include in future research campaigns higher amplitudes to know whether they could deliver more positive results and to gain understanding as to how the material is modified overall by the process. On the other hand, it is assumed that the combination of force and amplitude change depending on the material that is

being modified, and for that reason similar experimental works should be applied on further materials to reach an optimal combination of those parameters to maximize the mechanical properties of plates.

4. Conclusions

In this paper, it has been shown that ball burnishing affects the superficial hardening of S235JR steel plates, and that both the burnishing preload and the amplitude of the vibration to assist the process positively influence that increase. A method to evaluate the deep effect of the process, by performing a series of Vickers indentation tests using increasing loads, was proposed and validated. Indeed, it has been proven that the effect of ball burnishing is most purely represented if the Vickers indentations are performed with a 0.05 kg load, to minimize the inclusion of unaffected deep material in the measurement. Lower loads could lead to detrimental results due to experimental error.

Higher values of the burnishing preload have a positive effect in terms of mechanical properties ($Rp_{0.2}$, UTS, RM, σ_0, ϵ_p and n) shown by the material in tensile tests, although the vibration-assistance does not have an evident consequence on the modification of the material's behavior. That is, the combination of the core material and the hardened surface layer comprising the specimen's overall cross-section cancels out the effects of vibration-assistance of ball burnishing at a macro level. The deformation when necking occurs (e_{UTS}) is the only property that is hindered by ball burnishing, due to the fact that the process reduces the ductility of the material.

Overall, results have proven that although vibration-assisted ball burnishing is a finishing operation that affects the surface integrity of plates, it can affect, notably, the mechanical behavior of S235JR carbon steel, and can be considered as a feasible operation in these terms. However, it is also clear that the effect of vibration-assistance loses relevance as the burnishing preload is increased.

Author Contributions: Conceptualization, J.L. and G.G.-G.; methodology, J.L., G.G.-G., R.J.-M. and J.A.T.-R.; software, J.L.; validation, J.L., G.G.-G., R.J.-M. and J.A.T.-R.; formal analysis, J.L.; investigation, J.L. and J.R.-M.; resources, J.A.T.-R. and R.J.-M.; data curation, J.R.-M.; writing–original draft preparation, J.L.F.; writing–review and editing, R.J.-M.; supervision, G.G.-G.; project administration, J.A.T.-R.; funding acquisition, J.A.T.-R. and R.J.-M. All authors have read and agreed to the published version of the manuscript.

Funding: Financial support for this study was provided by the Ministry of Science, Innovation and Universities of Spain, through grant RTI2018-101653-B-I00, which is greatly appreciated. Additionally by the regional government of Catalonia and FEDER funds for regional development through grant IU68-016744.

Conflicts of Interest: The authors declare no conflict of interest..

Abbreviations

The following abbreviations are used in this manuscript:

A	Vibration amplitude
BB	Ball burnishing
e_{UTS}	Deformation at ultimate strength
F	Burnishing preload
FHD	Full high definition
HD	High definition
k	Strength index
n	Strain hardening coefficient
Ra	Average surface roughness
RM	Resilience module
$Rp_{0.2}$	Yield stress
UTS	Ultimate tensile strength
UVABB	Ultrasonic vibration-assisted ball burnishing
VABB	Vibration-assisted ball burnishing

References

1. Iswanto, P.; Yaqin, R.; Sadida, H. Influence of shot peening on surface properties and corrosion resistance of implant material AISI 316L. *Metalurgija* **2020**, *59*, 309–312.
2. Iswanto, P.; Maliwemu, E.; Malau, V.; Imaduddin, F.; Sadida, H. Surface roughness, hardness, and fatigue-corrosion characteristic of AISI 316L by shot peening. *Metalurgija* **2020**, *59*, 183–186.
3. Swirad, S.; Pawlus, P. The Effect of Ball Burnishing on Tribological Performance of 42CrMo4 Steel under Dry Sliding Conditions. *Materials* **2020**, *13*, 2127. [CrossRef] [PubMed]
4. Teimouri, R.; Amini, S.; Guagliano, M. Analytical modeling of ultrasonic surface burnishing process: Evaluation of residual stress field distribution and strip deflection. *Mater. Scie. Eng. A* **2019**, *747*, 208–224. [CrossRef]
5. García-Granada, A.A.; Gomez-Gras, G.; Jerez-Mesa, R.; Travieso-Rodriguez, J.A.; Reyes, G. Ball-burnishing effect on deep residual stress on AISI 1038 and AA2017-T4. *Mater. Manuf. Process.* **2017**, *32*, 1279–1289. [CrossRef]
6. Takada, Y.; Sasahara, H. Effect of tip shape of frictional stir burnishing tool on processed layer's hardness, residual stress and surface roughness. *Coatings* **2018**, *8*, 32. [CrossRef]
7. Estevez-Urra, A.; Llumà, J.; Jerez-Mesa, R.; Travieso-Rodriguez, J.A. Monitoring of Processing Conditions of an Ultrasonic Vibration-Assisted Ball-Burnishing Process. *Sensors* **2020**, *20*, 2562. [CrossRef]
8. Bozdana, A.T.; Gindy, N. Comparative experimental study on effects of conventional and ultrasonic deep cold rolling processes on Ti–6Al–4V. *Mater. Sci. Technol.* **2008**, *24*, 1378–1384. [CrossRef]
9. Gómez-Gras, G.; Travieso-Rodríguez, J.A.; González-Rojas, H.A.; Nápoles-Alberro, A.; Carrillo, F.J.; Dessein, G. Study of a ball-burnishing vibration-assisted process. *Proc. Inst. Mech. Eng. Part B J. Eng. Manuf.* **2015**, *229*, 172–177. [CrossRef]
10. Siu, K.; Ngan, A.; Jones, I. New insight on acoustoplasticity–ultrasonic irradiation enhances subgrain formation during deformation. *Int. J. Plasticity* **2011**, *27*, 788–800. [CrossRef]
11. Green, R. Non-linear effects of high-power ultrasonics in crystalline solids. *Ultrasonics* **1975**, *13*, 117–127. [CrossRef]
12. Amini, S.; Bagheri, A.; Teimouri, R. Ultrasonic-assisted ball burnishing of aluminum 6061 and AISI 1045 steel. *Mater. Manuf. Process.* **2018**, *33*, 1250–1259. [CrossRef]
13. Jerez-Mesa, R.; Landon, Y.; Travieso-Rodriguez, J.A.; Dessein, G.; Lluma-Fuentes, J.; Wagner, V. Topological surface integrity modification of AISI 1038 alloy after vibration-assisted ball burnishing. *Surf. Coat. Technol.* **2018**, *349*, 364–377. [CrossRef]
14. Travieso-Rodríguez, J.A.; Gras, G.G.; Peiró, J.J.; Carrillo, F.; Dessein, G.; Alexis, J.; Rojas, H.G. Experimental study on the mechanical effects of the vibration-assisted ball-burnishing process. *Mater. Manuf. Process.* **2015**, *30*, 1490–1497. [CrossRef]
15. Saldaña-Robles, A.; Plascencia-Mora, H.; Aguilera-Gómez, E.; Saldaña-Robles, A.; Marquez-Herrera, A.; Diosdado-De la Peña, J.A. Influence of ball-burnishing on roughness, hardness and corrosion resistance of AISI 1045 steel. *Surf. Coat. Technol.* **2018**, *339*, 191–198. [CrossRef]
16. Travieso-Rodriguez, J.A.; Gomez-Gras, G.; Dessein, G.; Carrillo, F.; Alexis, J.; Jorba-Peiro, J.; Aubazac, N. Effects of a ball-burnishing process assisted by vibrations in G10380 steel specimens. *Int. J. Adv. Manuf. Technol.* **2015**, *81*, 1757–1765. [CrossRef]
17. Pande, S.; Patel, S. Investigations on vibratory burnishing process. *Int. J. Mach. Tool Des. Res.* **1984**, *24*, 195–206. [CrossRef]
18. Pak, A.; Mahmoodi, M.; Safari, M. Experimental Investigation of the Effects of Initial Surface Roughness on Ultrasonic Assisted Ball Burnishing of Al6061-T6. *Modares Mech. Eng.* **2019**, *20*, 87–95.
19. Teimouri, R.; Amini, S.; Bami, A.B. Evaluation of optimized surface properties and residual stress in ultrasonic assisted ball burnishing of AA6061-T6. *Measurement* **2018**, *116*, 129–139. [CrossRef]
20. Rodríguez, A.; de Lacalle, L.L.; Celaya, A.; Lamikiz, A.; Albizuri, J. Surface improvement of shafts by the deep ball-burnishing technique. *Surf. Coat. Technol.* **2012**, *206*, 2817–2824. [CrossRef]
21. Huuki, J.; Hornborg, M.; Juntunen, J. Influence of ultrasonic burnishing technique on surface quality and change in the dimensions of metal shafts. *J. Eng.* **2014**, *2014*, 124247. [CrossRef]
22. Lu, L.; Sun, J.; Li, L.; Xiong, Q. Study on surface characteristics of 7050-T7451 aluminum alloy by ultrasonic surface rolling process. *Int. J. Adv. Manuf. Technol.* **2016**, *87*, 2533–2539. [CrossRef]

23. Jerez-Mesa, R.; Travieso-Rodriguez, J.A.; Gomez-Gras, G.; Lluma-Fuentes, J. Development, characterization and test of an ultrasonic vibration-assisted ball burnishing tool. *J. Mater. Process. Technol.* **2018**, *257*, 203–212. [CrossRef]
24. Jerez-Mesa, R.; Travieso-Rodríguez, J.A.; Landon, Y.; Dessein, G.; Lluma-Fuentes, J.; Wagner, V. Comprehensive analysis of surface integrity modification of ball-end milled Ti-6Al-4V surfaces through vibration-assisted ball burnishing. *J. Mater. Process. Technol.* **2019**, *267*, 230–240. [CrossRef]
25. Gomez-Gras, G.; Travieso-Rodriguez, J.A.; Jerez-Mesa, R.; Lluma-Fuentes, J.; de la Calle, B.G. Experimental study of lateral pass width in conventional and vibrations-assisted ball burnishing. *Int. J. Adv. Manuf. Technol.* **2016**, *87*, 363–371. [CrossRef]